0026-895X/00/050913-13$3.00/0
MOLECULAR PHARMACOLOGY

MOL 57:913–925, 2000 /13029/822096

^{125}I-α-Conotoxin MII Identifies a Novel Nicotinic Acetylcholine Receptor Population in Mouse Brain

PAUL WHITEAKER, J. MICHAEL MCINTOSH, SIQIN LUO, ALLAN C. COLLINS, and MICHAEL J. MARKS

Institute for Behavioral Genetics, University of Colorado, Boulder, Colorado (P.W., A.C.C., M.J.W.), and Departments of Biology (J.M.M., S.L.) and Psychiatry (J.M.M.), University of Utah, Salt Lake City, Utah.

Received October 18, 1999; accepted February 3, 2000

This paper is available online at http://www.molpharm.org

ABSTRACT

α-Conotoxin MII (CtxMII), a peptide toxin from the venom of the predatory cone snail *Conus magus*, displays an unusual nicotinic pharmacology. Specific binding of a radioiodinated derivative (^{125}I-α-CtxMII) was identified in brain region homogenates and tissue sections. Quantitative autoradiography indicated that ^{125}I-α-CtxMII binding sites have an unique pharmacological profile and distribution in mouse brain, being largely confined to the superficial layers of the superior colliculus, nigrostriatal pathway, optic tract, olivary pretectal, and mediolateral and dorsolateral geniculate nuclei. Expression of α-CtxMII binding sites in the nigrostriatal pathway, combined with evidence for α-CtxMII-sensitivity of nicotine-induced [^{3}H]dopamine release in rodent striatal preparations indicates that ^{125}I-α-CtxMII binding nicotinic acetylcholine receptors are likely to be physiologically important. Unlabeled α-CtxMII potently (K_i < 3 nM) competed for a subset of [^{3}H]epibatidine binding sites in mouse brain homogenates, but weakly (IC_{50} > 10 μM) interacted with ^{125}I-α-bungarotoxin and (−)-[^{3}H]nicotine binding sites, confirming this compound's novel nicotinic pharmacology. Quantitative autoradiography revealed that α-CtxMII binds with high affinity at a subset of [^{3}H]epibatidine binding sites with relatively low cytisine affinity ("cytisine-resistant" sites), resolving [^{3}H]epibatidine binding into three different populations, each probably corresponding to a receptor subtype. The majority population seems to correspond to that which binds nicotine and cytisine with high affinity ("cytisine-sensitive" sites). Comparison of the cytisine-resistant population's distribution with that of α3 subunit mRNA expression suggests that the fractions both more and less sensitive to α-CtxMII probably contain the α3 subunit, perhaps in combination with different β subunits.

Molecular cloning approaches have revealed the expression of 10 nicotinic acetylcholine receptor (nAChR) subunits [α2–α7, α9 (to date α8 has been identified only in avian neurons), and β2–β4] in mammalian neuronal tissue (Lindstrom et al., 1996). Each of the subunits' mRNA has a distinct pattern of expression, suggesting the possibility that they may mediate different processes. In the central nervous system, many of these neuronal nAChRs seem to be presynaptic, where they modulate the release of neurotransmitters such as dopamine, norepinephrine, acetylcholine, and γ-aminobutyric acid with differential pharmacologies (Wonnacott, 1997).

Heterologous expression of neuronal nAChR subunits has shown different subunit combinations (or expression of α7–α9 alone) result in functional nAChR subtypes with differing pharmacological and biophysical properties (Lindstrom et al., 1996). The number of neuronal nAChR subunits known theoretically allows the possibility of vast numbers of potential subunit combinations and receptor subtypes. However, efforts to discover which nAChR subtypes exist in the central nervous system (and their locations) have been hindered by the lack of subtype-specific pharmacological probes to identify individual subtypes within the mixed native nAChR population. Indeed, only two subtypes of neuronal nAChRs, those which correspond to ^{125}I-α-Bgt and 'high-affinity agonist binding' sites, have been thoroughly characterized so far. In mammalian neuronal systems, ^{125}I-α-Bgt is believed to bind largely (if not exclusively) to nAChRs containing the α7 subunit (Schoepfer et al., 1990; Seguela et al., 1992), whereas (−)-[^{3}H]nicotine, [^{3}H]cytisine, [^{3}H]acetylcholine, and [^{3}H]methylcarbamylcholine binding is only detectable at the α4β2 combination of subunits (Whiting and Lindstrom, 1987; Flores et al., 1992). Neuronal bungarotoxin (Bgt), a minor component of the venom of the Taiwanese banded krait *Bungarus multicinctus* (also named κ-Bgt, toxin F, and Bgt 3.1) showed initial promise as a selective antagonist of α3β2 subtype nAChRs (Luetje et al., 1990). However,

This work was supported by National Institute on Drug Abuse Grants DA12242, DA03194, and DA10156, National Institutes of Mental Health Grant MH53631, and National Institute of General Medical Sciences Grant GM48677. A.C.C. is supported, in part, by Research Scientist Award DA00197 from the National Institute on Drug Abuse.

ABBREVIATIONS: nAChR, nicotinic acetylcholine receptor; CtxMII, conotoxin MII; Bgt, bungarotoxin; PEI, polyethylenimine; Y_o-α-CtxMII, N-terminal tyrosine-tagged α-conotoxin MII; TFA, trifluoroacetic acid; SSC, standard saline citrate.

problems of availability (*B. multicinctus* is a protected species), complex kinetics of interaction at multiple nAChR subtypes (Papke et al., 1993), and the difficulty of ensuring the toxin's purity have severely restricted its usefulness. More recently, it has become apparent that the agonist ligand [^{3}H]epibatidine binds with detectable affinity to other neuronal nAChRs in addition to the $\alpha4\beta2$ subtype (Perry and Kellar, 1995; Marks et al., 1998; Parker et al., 1998), raising hopes of identifying further native nAChR populations.

α-CtxMII was identified in the venom of *Conus magus* by sequential fractionation and testing of the isolates for inhibition of $\alpha3\beta2$ nAChRs expressed in *Xenopus laevis* oocytes (Cartier et al., 1996). Experiments in native systems have demonstrated potent (nanomolar IC_{50} values) and selective blockade of nAChR subpopulations in rodent striatal (Grady et al., 1997; Kulak et al., 1997; Kaiser et al., 1998) and avian ciliary ganglion (Ullian et al., 1997) preparations. These functional studies provided strong evidence that α-CtxMII was a highly selective antagonist of a novel native receptor population. The high affinity and novel subtype selectivity of α-CtxMII make it a potentially useful ligand, particularly in light of its proven ability to interact with native neuronal nAChRs and the present paucity of selective pharmacological tools.

In this study, a radiolabeled version of α-CtxMII ([^{125}I]αCtxMII) was used to identify, locate, and enumerate α-CtxMII binding nAChRs in mouse brain. The distribution and pharmacology of these receptors differs from those previously characterized, indicating that they represent a novel population. Using unlabeled α-CtxMII in combination with existing nicotinic ligands allowed identification of α-CtxMII binding nAChRs as part of the set of high-affinity [^{3}H]epibatidine binding nAChRs, but distinct from the traditionally recognized "high-affinity agonist binding" $\alpha4\beta2$ subtype. The pharmacological characteristics and distribution of α-CtxMII binding nAChRs indicate that they are likely to be composed of (at least) α3 and β2 subunits.

Experimental Procedures

Animals. Male mice (C57BL/6J, 60–90 days old) were used throughout this study. Mice were bred at the Institute for Behavioral Genetics and housed five per cage. The vivarium was maintained on a 12-h/12-h light/dark cycle (lights on 7 AM to 7 PM), and mice were given free access to food and water. The Animal Care and Utilization Committee of the University of Colorado, Boulder, approved all procedures used in this study.

Materials. [^{3}H]Epibatidine (specific activity, 33.8 Ci/mmol), (−)-[^{3}H]nicotine (specific activity, 81.5 Ci/mmol), Na^{125}I (specific activity, 2200 Ci/mmol), and uridine triphosphate (α-^{35}S; initial specific activity, 800 Ci/mmol) were obtained from DuPont NEN (Boston, MA). ^{125}I-α-Bgt (initial specific activity, 230 Ci/mmol), Hyperfilm β-max, and Hyperfilm-^{3}H were purchased from Amersham (Mt. Prospect, IL). NaCl, NaOH, KCl, $MgCl_2$, $MgSO_4$, $CaCl_2$, chloramine T, ammonium acetate, lysozyme, Tris · HCl, sodium carbonate, sodium bicarbonate, polyethylenimine (PEI; 50% w/v solution), yeast tRNA, triethanolamine, sodium citrate, dithiothreitol, Denhardt's solution, acetic anhydride, diethylpyrocarbonate, sodium phosphate, gelatin, poly-L-lysine, chromium aluminum sulfate, BSA (Fraction V), phenylmethylsulfonyl fluoride, EDTA, EGTA, aprotinin, leupeptin trifluoroacetate, and pepstatin A were obtained from Sigma Chemical Co. (St. Louis, MO). (−)-nicotine bitartrate and DPX mountant were bought from BDH Chemicals (Poole, UK). Glass fiber filters Type A/E were obtained from Gelman Sciences (Ann Arbor, MI) and Type GB from MFS (Dublin, CA). Budget Solve scintillation fluid was purchased from RPI (Arlington Heights, IL). ATP, CTP, GTP, and RNase A were purchased from Boehringer-Mannheim (Indianapolis, IN). The enzymes SP6 RNA polymerase and *Hin*dIII, were obtained from Promega (Madison, WI). Dextran sulfate was purchased from Pharmacia (Uppsala, Sweden), and formamide from Fluka Chemical Corp. (Ronkonkoma, NY).

Preparation of α-CtxMII and Y_0-α-CtxMII and Iodination of Y_0-α-CtxMII. Unmodified α-CtxMII was synthesized as described previously (Cartier et al., 1996). To provide an iodination site, α-CtxMII was synthesized with the addition of a tyrosine at the N terminus (Y_0-α-CtxMII). Although the two histidine residues present in native MII also provide potential iodination sites, structure-function studies suggested that modification of these sites would lead to unacceptable levels of decreased toxin potency (G. E. Cartier, unpublished observations). Synthesis of Y_0-α-CtxMII was achieved by methods described previously (Cartier et al., 1996).

To iodinate the peptide, 25 nmol of Y_0-α-CtxMII was dissolved in 25 μl of H_2O. To this was added 40 μl of 0.3 M NH_4Ac, pH 5.3. Approximately 10 mCi of Na^{125}I (volume ~22 μl) was added. The iodination reaction was initiated by the addition of 40 μl of freshly prepared 0.4 mM chloramine T. The reaction proceeded at room temperature (~22°C) for 10 min and was then terminated by the addition of 65 μl of 0.5 M ascorbic acid. The pH of the reaction mix was further lowered by the addition of 0.8 ml of 0.1% trifluoroacetic acid (TFA). Mono- and di-iodinated peptides were separated from unmodified peptides by reversed-phase HPLC using an analytical Vydac C18 column. Buffer A was 0.1% TFA, buffer B was 0.09% TFA, 60% acetonitrile, and the loading loop size was 5 ml. The gradient was 25%-75% B over 50 min. Flow rate was 1 ml/min and absorbance was monitored at 220 nM. A solution of sodium thiosulfate (2.5%) and potassium iodide (0.2%) in 1 N NaOH was added to the waste collection beaker to trap unreacted ^{125}I. Fractions containing peptide were collected in polypropylene tubes containing 10 μl of 20 mg/ml lysozyme to decrease adsorption to the tubes. After collection, peptide material was lyophilized and resuspended in 100 μl of 40% MeOH. Under the above chromatographic conditions, the unmodified peptide elutes at approximately 27 min with monoiodo peptide eluting at approximately 29 min. Final yield (estimated from counting an aliquot in a gamma counter) was approximately 2 nmol of monoiodo peptide. Monoiodination of the N-terminal tyrosine was verified by chemical sequencing and mass spectrometry.

Quantitative Autoradiography of ^{125}I-α-CtxMII and [^{3}H]Epibatidine Binding. Quantitative autoradiography procedures were similar to those described previously (Pauly et al., 1989; Marks et al., 1998). Three C57BL/6J mice were sacrificed by cervical dislocation. The brains were removed from the skulls and rapidly frozen by immersion in isopentane (−35°C, 10 s). The frozen brains were wrapped in aluminum foil, packed in ice, and stored at −70°C until sectioning. Tissue sections (14 μm thick) prepared using an IEC Minotome Cryostat refrigerated to −16°C were thaw mounted onto subbed microscope slides (Richard Allen, Richland, MI). Slides were subbed by incubation with gelatin (1% w/v)/chromium aluminum sulfate (0.1% w/v) for 2 min at 37°C, drying overnight at 37°C, incubation at 37°C for 30 min in 0.1% (w/v) poly-L-lysine in 25 mM Tris, pH 8.0, and drying at 37°C overnight. Mounted sections were stored desiccated at −70°C until use. Eight series of sections were collected from each mouse brain.

Before incubation with ^{125}I-α-CtxMII, three adjacent series of sections from each mouse were incubated in binding buffer (144 mM NaCl, 1.5 mM KCl, 2 mM $CaCl_2$, 1 mM $MgSO_4$, 20 mM HEPES, 0.1% BSA (w/v), pH 7.5) + phenylmethylsulfonyl fluoride (1 mM, to inactivate endogenous serine proteases) at 22°C for 15 min. For all ^{125}I-α-CtxMII binding reactions, the standard binding buffer was supplemented with BSA [0.1% (w/v)], 5 mM EDTA, 5 mM EGTA, and 10 μg/ml each of aprotinin, leupeptin trifluoroacetate, and pepstatin A to protect the ligand from endogenous proteases. The sections were then incubated with 0.5 nM ^{125}I-α-CtxMII for 2 h at 22°C. The first

series of sections was used to determine total ^{125}I-α-CtxMII binding (no competing ligands), the second to measure cytisine-resistant ^{125}I-α-CtxMII binding (in the presence of 20 nM unlabeled cytisine), whereas the third series of sections from each mouse was used to determine nonspecific ^{125}I-α-CtxMII binding (in the presence of 1 μM unlabeled epibatidine). ^{125}I-α-CtxMII binding was further investigated by coincubation of sections with varying concentrations of unlabeled ligands (cytisine, 1–300 nM; epibatidine, 10–1000 pM; α-Bgt, 1 μM; (−)-nicotine, 30–3000 nM). After incubation with ^{125}I-α-CtxMII, the slides were washed as follows: 30 sec in binding buffer + 0.1% (w/v) BSA (22°C), 30 sec in binding buffer + 0.1% (w/v) BSA (0°C), 5 sec in 0.1× binding buffer + 0.01% (w/v) BSA (twice at 0°C), and twice at 0°C for 5 sec in 5 mM HEPES (pH 7.5).

Sections for use in [^{3}H]epibatidine binding were rehydrated in binding buffer at 22°C for 15 min, followed by incubation with 500 pM [^{3}H]epibatidine for 2 h at 22°C. Four series of adjacent sections were used from each mouse to measure total [^{3}H]epibatidine binding (no competing ligand), [^{3}H]epibatidine binding in the presence of 100 nM unlabeled cytisine, [^{3}H]epibatidine binding in the presence of 100 nM unlabeled cytisine + 50 nM unlabeled α-CtxMII, and nonspecific [^{3}H]epibatidine binding [in the presence of 1 mM unlabeled (−)-nicotine]. Concentrations of unlabeled cytisine and α-CtxMII were chosen on the basis of results obtained in this study from [^{3}H]epibatidine inhibition binding studies in membrane preparations (Fig. 4, right). Slides were washed by sequential incubation in the following buffers (all steps at 0°C): 5 sec in binding buffer (twice), 5 sec in 0.1× binding buffer (twice), and 5 sec in 5 mM HEPES, pH 7.5 (twice).

Sections were initially dried with a stream of air, then by overnight storage (22°C) under vacuum. Mounted, desiccated sections were apposed to film (1–3 days, Amersham Hyperfilm β-Max film for ^{125}I-labeled sections; 8 weeks, Amersham Hyperfilm-^{3}H for ^{3}H-labeled sections). To allow quantification, each film was also exposed to tissue paste standards of defined specific activity (Geary et al., 1985). For tritium, specific activities were 0.05 to 50 nCi/mg (wet weight), whereas for ^{125}I, specific activities were 0.25 to 60 nCi/mg (wet weight). The exact specific activities of the tissue paste standards were determined by measuring radioactivity in weighed aliquots.

After the films had been exposed to the sections for an appropriate length of time, they were developed and signal intensity in selected brain regions was measured by digital image analysis. Films were illuminated using a Northern Light light box, and autoradiographic images of the sections and tissue paste standards were captured using a CCD imager camera. Signal intensity was determined using NIH-Image 1.61. Where possible, six independent measurements from different tissue sections were made for each brain region, under each incubation condition, for each mouse. The absorbance measurements for each brain area were averaged, and the mean absorbance was used to calculate the degree of labeling by reference to the relevant standard curve.

Membrane Preparation. Each C57BL/6J mouse was sacrificed by cervical dislocation. The brain was removed from the skull and placed on an ice-cold platform. Brains were either dissected into 12 regions [olfactory bulbs, cerebellum, hindbrain (pons-medulla), hypothalamus, hippocampus, striatum, cerebral cortex, thalamus, midbrain, interpeduncular nucleus, superior colliculus, and inferior colliculus] or the hindbrain, cerebellum, and olfactory bulbs were discarded without further dissection ("whole brain" preparation). Samples were homogenized in ice-cold hypotonic buffer (14.4 mM NaCl, 0.2 mM KCl, 0.2 mM $CaCl_2$, 0.1 mM $MgSO_4$, 2 mM HEPES, pH 7.5) using a glass-Teflon tissue grinder. The particulate fractions were obtained by centrifugation at 20,000*g* (15 min, 4°C; Sorval RC-2B centrifuge). The pellets were resuspended in fresh homogenization buffer, incubated at 37°C for 10 min, then harvested by centrifugation as before. Each pellet was washed twice more by resuspension/centrifugation, then stored (in pellet form under homogenization buffer) at −70°C until used. Protein concentrations in the membrane preparations were measured using the method of Lowry et al. (1951), using BSA as the standard.

(−)-[^{3}H]Nicotine Binding to Membranes. The binding of (−)-[^{3}H]nicotine was measured using the method of Marks et al. (1986), modified for use with a 96-well plate washer. Membrane samples (200 μg of whole brain preparation) were incubated in 96-well polystyrene plates with 20 nM (−)-[^{3}H]nicotine in 100 μl of binding buffer for 30 min at 22°C. Binding reactions were terminated by filtration of samples onto PEI-soaked (0.5% w/v in binding buffer) glass fiber filters (types GFA/E and GB) using an Inotech Cell Harvester (Inotech, East Lansing, MI). Samples were subsequently washed six times with ice-cold binding buffer. Total and nonspecific [in the presence of 1 mM (−)-nicotine tartrate] binding were determined in triplicate. Where inhibition binding was being measured, various concentrations of competing ligands were included in triplicate wells.

^{125}I-α-Bgt Binding to Membranes. Binding of ^{125}I-α-Bgt to membrane preparations was performed using procedures similar to those used with (−)-[^{3}H]nicotine, except that incubation times were extended to 5 h and samples contained 1 nM ^{125}I-α-Bgt instead of 20 nM (−)-[^{3}H]nicotine. The GFA/E filters were treated with 0.5% PEI and the GFB filters were treated with 5% (w/v) nonfat dry milk before filtration.

[^{3}H]Epibatidine Binding to Membranes. Binding of [^{3}H]epibatidine was quantified as described previously (Marks et al., 1998). Incubations were performed in 1-ml polypropylene tubes in a 96-well format, using 50 to 200 μg of membrane protein per tube (depending on brain region). A 500-μl reaction volume was used to minimize problems of ligand depletion, and all incubations progressed for 2 h at 22°C. The concentration of [^{3}H]epibatidine (500 pM) used in inhibition binding experiments was chosen to maintain binding of ligand to the tissue at 5% or less of total ligand added. Saturation binding experiments were performed for membrane preparations from each brain region, using ligand concentrations in the range 10 to 800 pM. At the lower concentrations, a significant proportion of ligand bound to the tissue. Free [^{3}H]epibatidine concentrations were estimated by correcting for the amount of ligand bound to tissue, and these corrected concentrations were used to calculate K_d values for [^{3}H]epibatidine binding in each brain region and, thus, the K_i values for each compound versus [^{3}H]epibatidine binding.

^{125}I-α-CtxMII Binding to Membranes. Large amounts of nonspecific binding were seen when using ^{125}I-α-Ctx (0.2–32 nM) in filtration binding assays. Best assay performance was produced using the following modifications to the (−)-[^{3}H]nicotine binding procedure. Incubation times were extended to 2 h, and incubation buffer was supplemented with BSA [0.1% (w/v)], 5 mM EDTA, 5 mM EGTA, and 10 μg/ml each of aprotinin, leupeptin trifluoroacetate, and pepstatin A to protect the ligand from endogenous proteases. The glass fiber filters were treated with 5% (w/v) nonfat dry milk before filtration.

In Situ RNA Hybridization. The method used for in situ hybridization using riboprobes was identical with that used by Simmons et al. (1989) and Marks et al. (1992). Probes were prepared by in vitro transcription, using α-^{35}S-UTP as the sole source of UTP. The α3 probe was prepared from clone pPCA48E(4) cloned in pSP65, linearized using *Hin*dIII, and synthesized using SP6 RNA polymerase. The synthesis was designed to yield full-length antisense transcript. Immediately before hybridization, the probe was subjected to alkaline hydrolysis using the method of Cox et al. (1984) to yield products with average sizes of 500 bases.

After hybridization, slides were air dried and stored under vacuum overnight before exposure to Amersham Hyperfilm β-Max film (10 days). To allow α3 hybridization to be quantified, the film was also exposed to a set of dot-blotted ^{35}S standards. Serial dilutions of the [^{35}S]cRNA were made in 5× standard saline citrate (SSC; 1× SSC, 150 mM NaCl, 15 mM trisodium citrate, pH 7.0, with HCl), and 400 μl of each dilution was applied to a prewetted (5× SSC) nylon membrane (New England Nuclear, Beverly, MA) by vacuum filtra-

tion through a 96-well manifold (Life Technologies, Bethesda, MD). The samples were washed three times with 5× SSC and allowed to dry at room temperature. One set of the dilution series was cut from the membrane and counted on a liquid scintillation counter to determine exact counts per unit area. Standards ranged from 0.1 to 60 pCi/mm^2. After exposure to the sections and standards, the films were developed. Autoradiographic images were captured and hybridization densities quantified as described above for autoradiographic analysis of ligand binding.

Calculations. Results for saturation binding experiments were calculated using the Hill equation: $B = B_{max}\, L^n / (L^n + K_d^n)$, where B is the binding at the free ligand concentration L, B_{max} is the maximum number of binding sites, K_d is the equilibrium binding constant, and n is the Hill coefficient. Values of B_{max}, K_d, and n were calculated using the nonlinear least-squares fitting algorithm of Sigma Plot version 5.0 (Jandel Scientific, San Rafael, CA). Results for inhibition of (−)-[^{3}H]nicotine and ^{125}I-α-Bgt binding were calculated using a one-site fit: $B = B_o / [1 + (I / IC_{50})]$ where B is ligand bound at inhibitor concentration I, B_o is the binding in the absence of inhibitor, and IC_{50} is the concentration of inhibitor required to reduce binding to 50% of B_o. Results for inhibition of ligand binding were calculated using the formulae for either one (as above) or two binding sites: $B = B_1 / [1 + (I / IC_{50-1})] + B_2 / [1 + (I / IC_{50-2})]$, where B is ligand bound at inhibitor concentration I, and B_1 and B_2 are binding sites sensitive to inhibition with IC_{50-1} and IC_{50-2}, respectively. Values for K_i (inhibition binding constant) were derived by the method of Cheng and Prusoff (1973): $K_i = IC_{50} / 1 + (L / K_d)$.

Results

^{125}I-α-CtxMII Autoradiography, Mouse Brain Sections. Preliminary experiments (using monoiodinated but nonradioactive Y_0-α-CtxMII) showed that it remained a potent inhibitor at α3β2 nAChRs expressed in *X. laevis* oocytes (K_d = 1.9 nM, compared with 0.35 nM for the native toxin; data not shown). In light of these data, attempts were made to identify specific, nicotinic α-CtxMII binding using the monoradioiodinated version of this ligand (^{125}I-α-CtxMII) in mouse brain sections.

To minimize nonspecific binding, and reduce the possibility of labeling lower-affinity receptor populations, a low (0.5 nM) concentration of ^{125}I-α-CtxMII was used in autoradiography experiments. Under these conditions, a small amount of tissue mediated nonspecific binding of ^{125}I-α-CtxMII binding (defined in the presence of 1 μM unlabeled epibatidine) was seen. However, specific ^{125}I-α-CtxMII binding could be clearly distinguished over the tissue background (Fig. 1). Minor variations in nonspecific binding were noted, making it necessary to measure nonspecific binding in each individual region to ensure accurate quantification of specific signal strength. Subsequent experiments showed that using higher ^{125}I-α-CtxMII concentrations produced unacceptably high levels of nonspecific binding. Monoiodination produced radiolabeled toxin of high specific activity (2200 Ci/mmol), allowing short film exposures (24–72 h). Toxin was used through one half-life without any detectable increase in nonspecific signal or decrease in specific signal strength.

The highest levels of specific ^{125}I-α-CtxMII binding [>5 fmol/mg (wet weight)] were detected in the dorsolateral and ventrolateral geniculate nuclei, olivary pretectal nucleus, and the zonal layer of the superior colliculus. High levels (4–5 fmol/mg) of ^{125}I-α-CtxMII binding were also detected in the superficial gray of the superior colliculus and in the oculomotor nerve. Outside these highly labeled regions, binding densities were lower and sites were mainly found in nigrostriatal and optic-tract-associated regions, as summarized in Table 1.

The distribution of specific ^{125}I-α-CtxMII binding resembled a subset of the cytisine-resistant high affinity [^{3}H]epibatidine binding population reported by Marks et al. (1998). The abilities of unlabeled epibatidine, cytisine, α-Bgt, and nicotine to compete for ^{125}I-α-CtxMII-binding sites were measured by quantitative autoradiography. Competition binding was assessed in striatum and the superficial gray of the superior colliculus, as most of the other regions containing ^{125}I-α-CtxMII binding are too small to allow sufficient tissue slices to be collected. Even high concentrations of α-Bgt (1 μM) had no effect on ^{125}I-α-CtxMII-binding. In contrast, all three of the remaining ligands competed effectively

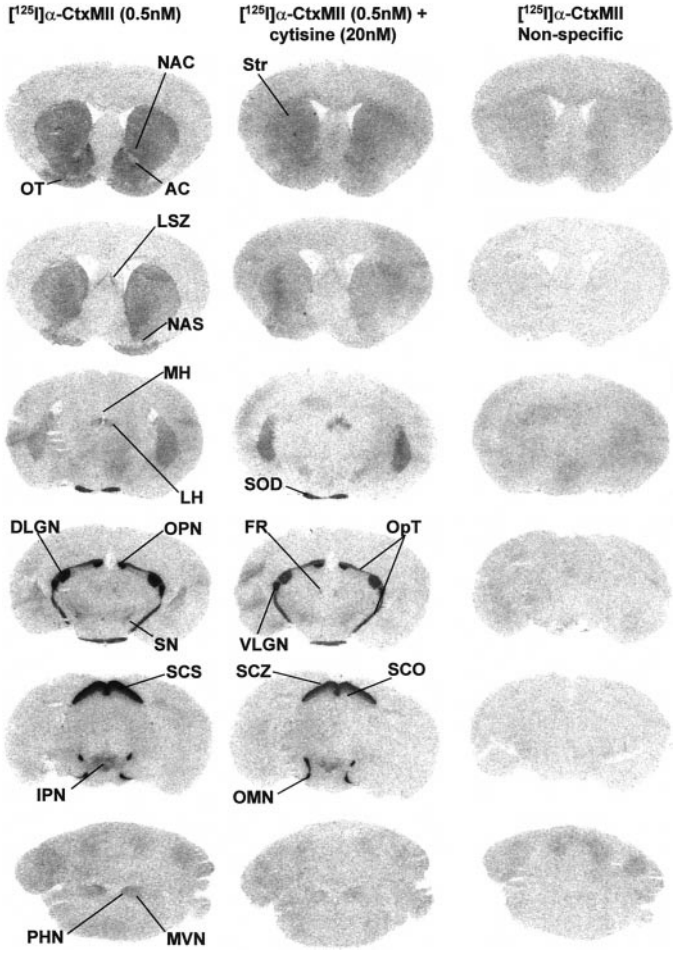

Fig. 1. Autoradiographic representation of ^{125}I-α-CtxMII binding in mouse brain [total, with cytisine (20 nM), and nonspecific]. Sections (14 μm) were incubated with 0.5 nM ^{125}I-α-CtxMII alone (left column), in the presence of 20 nM cytisine (center column), and with 1 μM epibatidine (nonspecific ^{125}I-α-CtxMII; right column) as described under *Experimental Procedures*. The sections are adjacent in each row, and the panels are digital images of autoradiograms. The abbreviations used to identify brain regions are: AC, anterior commissure; DLGN, dorsolateral geniculate nucleus; FR, fasciculus retroflexus; IPN, interpeduncular nucleus; LH, lateral habenula; LSZ, lambdoid septal zone; MH, medial habenula; MVN, medial vestibular nucleus; NAC, nucleus accumbens core; NAS, nucleus accumbens shell; OMN, oculomotor nerve (or root); OPN, olivary pretectal nucleus; Opt, optic tract; OT, olfactory tubercle; PHN, prepositus hypoglossal nucleus; SCO, superior colliculus, optic nerve layer; SCS, superior colliculus, superficial gray; SCZ, superior colliculus, zonal layer; SN, substantia nigra; SOD, supraoptic decussation; Str, striatum; VLGN, ventrolateral geniculate nucleus.

for ^{125}I-α-CtxMII-binding in a monophasic manner (Fig. 2). Assuming a K_d value of 1.9 nM for ^{125}I-α-CtxMII-binding (obtained in competition binding experiments using nonradioactive, monoiodinated Y_0-α-CtxMII, as mentioned previously), K_i values in the superficial gray of the superior colliculus were epibatidine, 81 ± 32 pM; cytisine, 14 ± 6 nM; and (−)-nicotine, 381 ± 43 nM, whereas the corresponding values in the striatum were epibatidine, 89 ± 30 pM; cytisine, 18 ± 4 nM; and (−)-nicotine, 276 ± 67 nM. Hill coefficients were not significantly different from 1 for each drug in each region (Fig. 2).

To determine whether ^{125}I-α-CtxMII binding sites nAChRs are uniformly cytisine resistant, the cytisine sensitivity of ^{125}I-α-CtxMII binding was assessed by addition of 20 nM cytisine to the binding buffer (a concentration that the previous workers' data indicated would abolish binding to cytisine-sensitive [^{3}H]epibatidine binding nAChRs). Binding of ^{125}I-α-CtxMII (0.5 nM) was noticeably diminished by coincubation with cytisine (20 nM) but was not reduced to background levels (Fig. 1; Table 1). Comparison of ^{125}I-α-CtxMII binding densities in the presence and absence of cytisine showed that across brain regions, addition of 20 nM cytisine reduced ^{125}I-α-CtxMII binding by an average of 40% (Table 1, right column; Fig. 3). In all regions where it was detectable, specific ^{125}I-α-CtxMII binding displayed the same cytisine sensitivity (correlation analysis showed $r = 0.96$; Fig. 3).

To extend the preceding findings, attempts were made to identify specific, nicotinic α-CtxMII binding using ^{125}I-α-CtxMII in regionally dissected brain tissue. However, high nonspecific binding (presumably to the brain homogenates) was observed even under optimized conditions (see *Experimental Procedures*; approximately 2% of the ligand added was retained as nonspecific binding when using 100 μg of protein/well of membranes). The autoradiography data suggested that superior colliculus membranes should contain the highest density of ^{125}I-α-CtxMII binding sites; indeed, evidence for specific, nicotinic binding of ^{125}I-α-CtxMII (displaceable by 1 μM epibatidine) was observed in superior colliculus membrane preparations. Interassay variation in total and nonspecific binding was substantial, but intra-assay variation was more manageable and each individual experiment using superior colliculus membranes provided evidence for specific binding above the nonspecific binding recorded. Fitting to a Hill binding curve indicated a B_{max} of 60 ± 21 fmol/mg of protein, a K_d of 4.9 ± 3.3 nM, and a Hill coefficient of 1.09 ± 0.34 (mean ± S.E.M. of five separate determinations). No evidence for specific ^{125}I-α-CtxMII binding could be obtained in the other brain regions tested, presumably because of the lower densities of binding sites in these regions.

(−)-[^{3}H]Nicotine, ^{125}I-α-Bgt and [^{3}H]Epibatidine Binding, Mouse Brain Membrane Preparations. To ex-

TABLE 1

Regional distribution of specific mouse brain ^{125}I-α-CtxMII binding in the presence and absence of 20 nM cytisine.

Mouse brain sections (14 μm) were incubated in the presence of ^{125}I-α-CtxMII (0.5 nM) with or without 20 nM cytisine. Binding of ^{125}I-α-CtxMII was detected by exposing βmax film to the sections, followed by digital densitometry of the autoradiographic images. Amounts of ligand bound were calculated by reference to ^{125}I-containing tissue paste standards. Because levels of ^{125}I-α-CtxMII nonspecific binding varied noticeably between brain regions, nonspecific binding was determined in each region, and was used to calculate specific binding (presented in terms of femtomoles of ^{125}I-α-CtxMII bound per milligram of tissue weight). Measurements were made six times in each region, in each mouse, where possible. Values are the mean ± S.E. of binding measured in three different mice.

	Total ^{125}I-α-CtxMII Binding	^{125}I-α-CtxMII Binding with Cytisine (20 nM)	% Cytisine-Resistant (of total)
	fmol/mg wet wt.		
Telencephalon			
Neocortex			
Olfactory tubercles	0.58 ± 0.05	0.11 ± 0.03	18.9
Basal ganglia			
Nucleus accumbens, core	1.44 ± 0.07	0.66 ± 0.06	45.8
Nucleus accumbens, shell	0.86 ± 0.04	0.39 ± 0.03	45.3
Striatum	0.81 ± 0.02	0.38 ± 0.07	46.9
Substantia nigra	0.75 ± 0.19	0.39 ± 0.13	52.0
Ventral tegmental area	1.29 ± 0.06	0.96 ± 0.11	74.4
Septum			
Lambdoid septal zone	0.82 ± 0.13	0.34 ± 0.08	41.5
Diencephalon			
Metathalamus			
Dorsolateral geniculate nucleus	5.00 ± 0.20	2.55 ± 0.26	51.0
Olivary pretectal nucleus	5.97 ± 0.12	3.20 ± 0.39	53.6
Ventrolateral geniculate nucleus	5.84 ± 0.18	3.31 ± 0.29	56.7
Epi- and subthalamus			
Lateral habenula	0.83 ± 0.11	0.43 ± 0.03	51.8
Medial habenula	1.11 ± 0.05	0.68 ± 0.07	61.3
Mesencephalon			
Interpeduncular nucleus	1.38 ± 0.04	1.05 ± 0.03	76.1
Superior colliculus, optic nerve layer	1.21 ± 0.03	0.65 ± 0.03	53.7
Superior colliculus, superficial grey	4.13 ± 0.01	2.23 ± 0.10	54.0
Superior colliculus, zonal layer	5.33 ± 0.10	3.47 ± 0.06	65.1
Pons			
Medial vestibular nucleus	0.50 ± 0.04	0.15 ± 0.02	30.0
Prepositus hypoglossal nucleus	0.56 ± 0.05	0.39 ± 0.06	69.6
Fiber Tracts			
Anterior commissure, anterior	0.26 ± 0.07	0.03 ± 0.03	11.5
Fasciculus retroflexus	0.80 ± 0.15	0.58 ± 0.07	72.5
Oculomotor nerve (or root)	4.71 ± 0.56	3.52 ± 0.25	74.7
Optic tract/brachium superior colliculus	2.66 ± 0.15	1.66 ± 0.19	62.4
Supraoptic decussation	2.48 ± 0.04	1.44 ± 0.15	58.1

pand on the data provided by ^{125}I-α-CtxMII competition binding experiments, the ability of α-CtxMII to displace (−)-[^{3}H]nicotine, ^{125}I-α-Bgt, and [^{3}H]epibatidine binding to mouse brain membrane preparations was assessed. For comparison, the ability of the nicotinic agonist cytisine to inhibit binding of the same ligands was also measured.

Inhibition of (−)-[^{3}H]nicotine (20 nM) and ^{125}I-α-Bgt (1 nM) binding (to α4β2 and α7 nAChRs, respectively) was measured in whole-brain membrane preparations. Cytisine produced a monophasic inhibition of both (−)-[^{3}H]nicotine and ^{125}I-α-Bgt binding (Fig. 4) but was much more potent in its interaction with the former (K_i = 0.36 ± 0.04 nM and 1.1 ± 0.5 μM, respectively). In contrast, α-CtxMII was only a weak inhibitor of (−)-[^{3}H]nicotine and ^{125}I-α-Bgt binding (K_i > 10 μM in each case).

Filtration binding was used to measure cytisine and α-CtxMII inhibition of [^{3}H]epibatidine binding in membrane preparations from 12 brain regions. Levels of [^{3}H]epibatidine binding varied widely among brain regions (Table 2). Levels were particularly high in the interpeduncular nucleus, with large amounts of [^{3}H]epibatidine binding also detected in superior colliculus and thalamic membranes. The lowest amounts of binding were found in the cerebellum and olfactory bulbs. As reported previously (Marks et al., 1998), saturation binding analysis provided [^{3}H]epibatidine binding K_d values of 20 to 40 pM in each region investigated, with no evidence for multiphasic ligand binding (data not shown). Also matching the results of Marks et al. (1998), cytisine inhibition of [^{3}H]epibatidine binding exhibits two phases (with K_I = 0.27 ± 0.05 nM and 32 ± 6 nM: "cytisine-sensitive" and "cytisine resistant," respectively), indicating that [^{3}H]epibatidine binds to receptor populations with differential cytisine affinity (but similar affinities for [^{3}H]epibatidine, according to the saturation binding profiles).

In the majority of regions surveyed, the more cytisine-sensitive phase of [^{3}H]epibatidine binding [believed to correspond to the high-affinity (−)-[^{3}H]nicotine binding site (Marks et al., 1998)] predominated. However, in olfactory bulb and interpeduncular nucleus preparations, the density of binding sites less sensitive to cytisine inhibition equaled or exceeded that of the cytisine-sensitive fraction (50% and 62% of [^{3}H]epibatidine binding in the two regions, respectively). Hippocampal membranes contained only cytisine-sensitive [^{3}H]epibatidine binding. Binding of [^{3}H]epibatidine was not detectably inhibited by α-CtxMII in interpeduncular nucleus, hindbrain, olfactory bulb, hippocampal, or cerebellar membranes. However, it is important to note that these region's small size (interpeduncular nucleus) or low overall receptor densities (hippocampus, hindbrain, olfactory bulb, and cerebellum) resulted in low numbers of total [^{3}H]epibatidine counts being retained, so minor populations of α-CtxMII-sensitive [^{3}H]epibatidine binding sites may have been overlooked. In contrast, α-CtxMII potently [K_i = 2.7 ± 1.3 nM (mean ± S.E.M. of values in the seven regions where α-CtxMII competition was observed); Table 2] inhibited a fraction of [^{3}H]epibatidine binding in the remaining brain regions studied. At the concentrations studied (30 pM-300 nM), α-CtxMII inhibition of [^{3}H]epibatidine binding appeared monophasic. The α-CtxMII-sensitive fraction of [^{3}H]epibatidine binding was approximately equal to the cytisine-resistant portion in the superior colliculus, striatum, and olfactory tubercles but was smaller in the remaining brain regions. Statistical analysis showed no significant differences in K_i values between regions for α-CtxMII inhibition

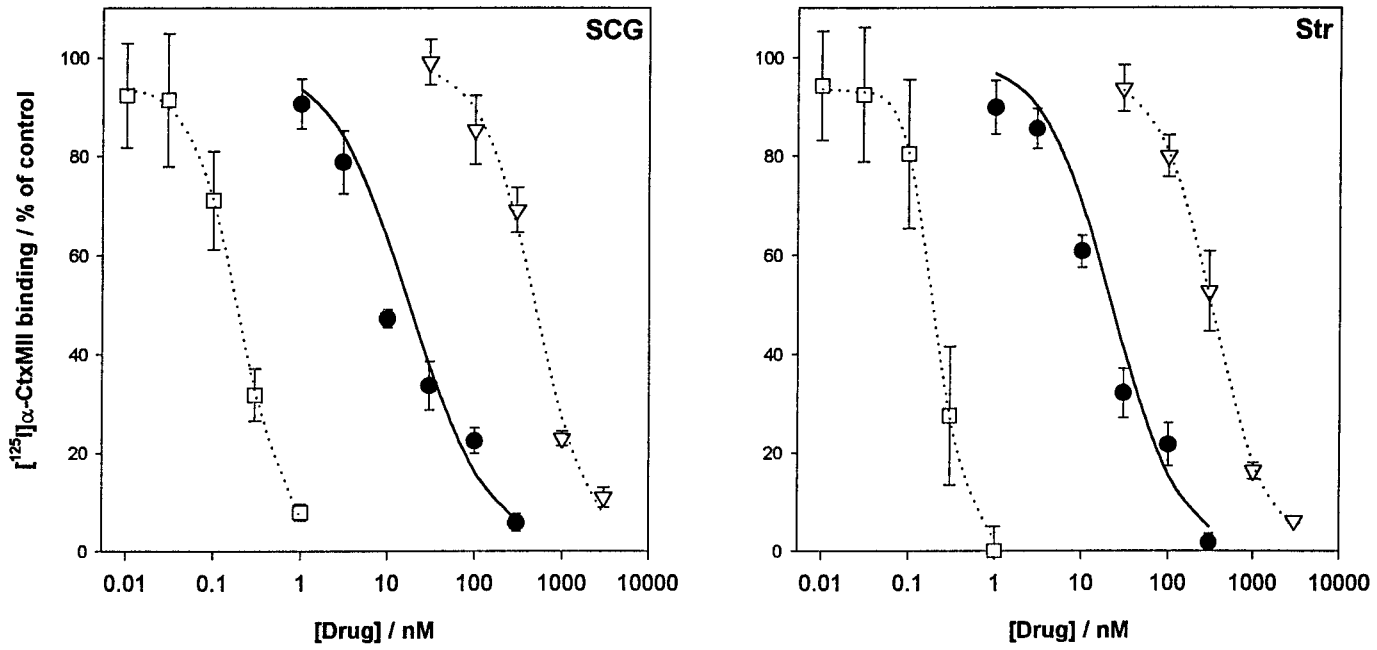

Fig. 2. Competition by cytisine, epibatidine, (−)-nicotine, and α-Bgt for ^{125}I-α-CtxMII binding sites in mouse brain. Sections (14 μm) were incubated with 0.5 nM ^{125}I-α-CtxMII in the presence of varying unlabeled ligand concentrations as described in the Methods section. Left, competition for specific ^{125}I-α-CtxMII binding in the superficial gray of the superior colliculus by epibatidine (□, IC_{50} = 103 ± 41 pM, n_H = −0.87 ± 0.09), cytisine (●, IC_{50} = 18 ± 8 nM, n_H = −0.94 ± 0.12), and (−)-nicotine (△, IC_{50} = 481 ± 54 nM, n_H = −1.47 ± 0.20). Right, competition for specific ^{125}I-α-CtxMII binding in the striatum by epibatidine (□, IC_{50} = 112 ± 38 pM, n_H = −0.80 ± 0.23), cytisine (●, IC_{50} = 23 ± 9 nM, n_H = −1.12 ± 0.17), and (−)-nicotine (△, IC_{50} = 348 ± 84 nM, n_H = −1.05 ± 0.24). α-Bgt (1 μM) did not displace ^{125}I-α-CtxMII binding in either region. Nonspecific binding was determined in the presence of 1 μM unlabeled epibatidine. Each point and value is the mean ± S.E.M. of four or five separate determinations. Data were fitted to a one-site Hill inhibition equation (see *Experimental Procedures*).

of [^{3}H]epibatidine binding (one-way ANOVA; $F(6,13) = 2.64$, $P > .05$). Displacement of [^{3}H]epibatidine binding to superior colliculus membranes by cytisine and α-CtxMII is shown in Fig. 4, right, whereas the regional distribution of total, cytisine-resistant, and α-CtxMII-sensitive specific [^{3}H]epibatidine binding is summarized in Table 2.

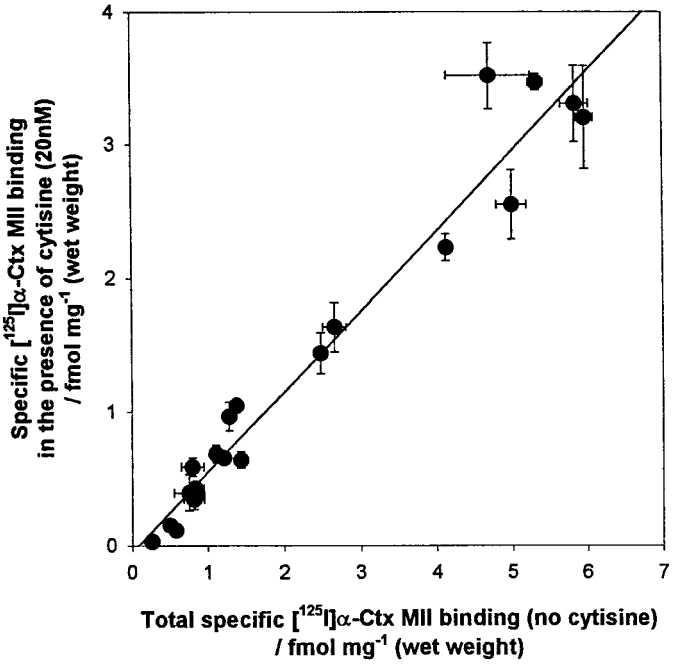

Fig. 3. Regional comparison of mouse brain-specific ^{125}I-α-CtxMII binding in the presence and absence of cytisine (20 nM). Levels of specific ^{125}I-α-CtxMII (0.5 nM) binding with and without the addition of 20 nM cytisine were determined by quantitative autoradiography and compared in 23 different brain regions. Each point is the mean ± S.E.M. of data gathered from three different animals. Linear regression showed $r = 0.96$, slope = 0.600.

[^{3}H]Epibatidine Autoradiography, Mouse Brain Sections. Competition binding experiments demonstrated that α-CtxMII was able to potently displace a fraction of [^{3}H]epibatidine binding to mouse brain membrane preparations. In addition, the same data showed that the density of α-CtxMII-sensitive [^{3}H]epibatidine binding sites varied widely among regions. Because the proportion of α-CtxMII-sensitive [^{3}H]epibatidine binding never exceeded that of the cytisine-resistant population (and in many regions was lower), it seemed possible that α-CtxMII was selectively interacting with a subpopulation of cytisine-resistant [^{3}H]epibatidine binding nAChRs, as suggested by the earlier ^{125}I-α-CtxMII autoradiography experiments. Crude regional dissection of the mouse brain provided limited anatomical resolution, so the relationship between cytisine-resistant and α-CtxMII-sensitive [^{3}H]epibatidine binding sites was explored using an autoradiographic approach. Inhibition binding experiments conducted using filtration binding indicated that 100 nM cytisine would essentially eliminate [^{3}H]epibatidine binding to cytisine-sensitive sites (at a [^{3}H]epibatidine concentration of 500 pM) but would leave the cytisine-resistant [^{3}H]epibatidine binding largely unaffected (Fig. 4, right). For this reason, cytisine-resistant [^{3}H]epibatidine binding was visualized using 500 pM [^{3}H]epibatidine, in combination with 100 nM cytisine. The same series of experiments also suggested that 50 nM α-CtxMII would be sufficient to displace α-CtxMII-sensitive [^{3}H]epibatidine binding, without affecting binding to other types of [^{3}H]epibatidine binding sites.

[^{3}H]Epibatidine proved to be an excellent autoradiographic probe, producing nonspecific binding that was indistinguishable from the film background. As would be anticipated from

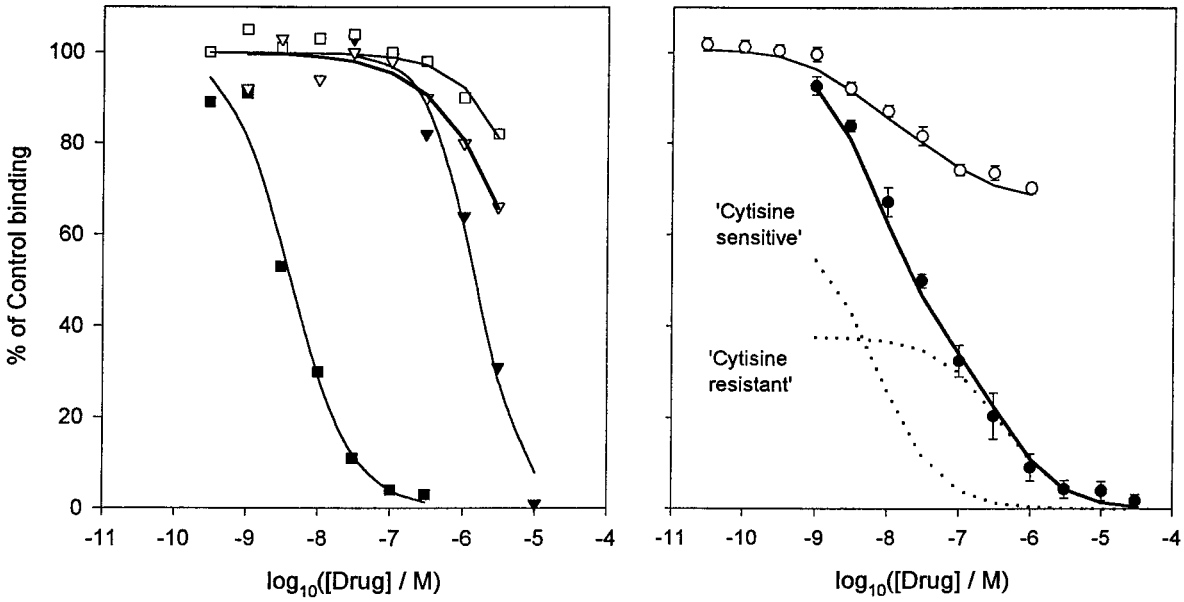

Fig. 4. Competition by cytisine and α-CtxMII for (−)-[^{3}H]nicotine, ^{125}I-α-Bgt and [^{3}H]epibatidine binding sites in mouse brain membranes. Left, mouse whole brain particulate fractions were incubated at 22°C with (−)-[^{3}H]nicotine (20 nM, 30 min; squares) or ^{125}I-α-Bgt (1 nM, 5 h; triangles) in the presence of unlabeled cytisine (1 nM - 10 μM; filled symbols) or α-CtxMII (1 nM - 10 μM; open symbols). Right, mouse superior colliculus particulate fractions were incubated at 22°C with [^{3}H]epibatidine (500 pM, 2 h; circles) in the presence of unlabeled cytisine (1 nM - 30 μM; filled symbols) or α-CtxMII (30 pM-3 μM; open symbols). Nonspecific binding was determined in the presence of 1 mM unlabeled (−)-nicotine. Each point represents the mean ± S.E.M. of three separate determinations. Data were fitted to either one- or two-site (for cytisine inhibition of [^{3}H]epibatidine binding) Hill inhibition equations (see *Experimental Procedures*). Both cytisine-sensitive and cytisine-resistant components of [^{3}H]epibatidine binding are illustrated on the right (dotted lines).

the competition binding experiments, most [^{3}H]epibatidine binding to mouse brain sections was cytisine-sensitive. In some regions (cingulate and frontal cortex, subiculum, reticular nuclei, dentate gyrus, and pontine nuclei) the addition of 100 nM cytisine abolished >96% of specific [^{3}H]epibatidine binding. In contrast, a small number of brain regions (accessory olfactory bulbs, interpeduncular nucleus, medial and lateral habenula, and fasciculus retroflexus) contained a majority of cytisine-resistant [^{3}H]epibatidine binding sites. These regions also contained the highest absolute densities of cytisine-resistant [^{3}H]epibatidine binding (Fig. 5; Table 3). In addition to these regions, cytisine-resistant [^{3}H]epibatidine binding was particularly distinct in the supraoptic decussation, optic tract, mediolateral and ventrolateral geniculate nuclei, olivary pretectal nucleus, and the superior and inferior colliculi. Where direct comparisons were possible, proportions of cytisine-resistant [^{3}H]epibatidine binding measured by quantitative autoradiography and filtration binding were in good agreement (interpeduncular nucleus, 60.1% by autoradiography, 62.4% by filtration binding; striatum, 8.0% by autoradiography, 13.6% by filtration binding; olfactory tubercles, 19.7% by autoradiography, 21.9% by filtration binding).

Addition of α-CtxMII (50 nM) resulted in a loss of [^{3}H]epibatidine binding from the cytisine-resistant population (defined in the presence of 100 nM cytisine). This loss was particularly noticeable in the superficial layers of the superior colliculus, the optic tract, supraoptic decussation, mediolateral and ventrolateral geniculate nuclei, the olivary pretectal nucleus, striatum, olfactory tubercles, and oculomotor nerve, where ≥ 75% of cytisine-resistant [^{3}H]epibatidine binding was α-CtxMII-sensitive. In contrast, in regions such as the inferior colliculus, interpeduncular nucleus, olfactory bulbs, medial habenula, and fasciculus retroflexus, much less α-CtxMII sensitivity was seen (Fig. 5; Table 3). Again, the distribution of α-CtxMII-sensitive [^{3}H]epibatidine binding established by quantitative autoradiography paralleled that measured by inhibition binding and ^{125}I-α-CtxMII autoradiography experiments.

Levels of specific ^{125}I-α-CtxMII binding were compared with those of α-CtxMII-sensitive [^{3}H]epibatidine binding (Fig. 6). In the majority of regions in which specific ^{125}I-α-CtxMII binding was seen, the two measures were highly correlated (r = 0.98; slope = 2.6). However, in six regions (medial habenula, lateral habenula, oculomotor nerve, zonal layer of the superior colliculus, fasciculus retroflexus, and interpeduncular nucleus), levels of α-CtxMII-sensitive [^{3}H]epibatidine binding fell above the correlation line. In each of these regions, autoradiography showed that in addition to detectable levels of specific ^{125}I-α-CtxMII binding, substantial amounts of [^{3}H]epibatidine binding less sensitive to both cytisine and unlabeled α-CtxMII were found.

α3 Subunit Expression: In Situ Hybridization. A previous investigation (Marks et al., 1998) suggested that cytisine-resistant [^{3}H]epibatidine binding is found in regions that express α3 nAChR subunit mRNA or in regions innervated by those that do. To explore this link more thoroughly, the distribution of α3 mRNA was mapped by in situ hybridization, and compared with that of cytisine-resistant [^{3}H]epibatidine binding. Hybridization was performed in brain slices prepared from the same animals used for autoradiographic investigations of ligand binding in this study, allowing direct comparisons to be made.

The pattern of α3 hybridization is shown in Fig. 5 (right column). Expression of α3 mRNA was restricted to a number of small, well-defined nuclei distributed throughout the brain. By far the highest level of hybridization was detected in the medial habenula (48 pCi/mm^2), the next highest amount (10 pCi/mm^2) being found in the mitral layer of the accessory olfactory bulbs. Where detected, hybridization in other brain regions was much weaker than in these two regions (3.2–0.6 pCi/mm^2). The distribution of α3 hybridization is summarized in Table 4. The highest densities of cytisine-resistant [^{3}H]epibatidine binding were found in the medial habenula and accessory olfactory bulbs, matching the data for α3 mRNA expression. In addition, patterns of α3 hybridization and cytisine-resistant [^{3}H]epibatidine binding were superimposed in many brain regions (including the dorsal cortex of the inferior colliculus, medial habenula, medial geniculate nucleus, superficial layers of the superior colliculus, and the medial vestibular and prepositus hypoglossal nuclei). In other cases, cytisine-resistant [^{3}H]epibati-

TABLE 2

[^{3}H]Epibatidine binding: cytisine-resistant and α-CtxMII-sensitive populations in 12 brain regions

Particulate fractions were prepared from the indicated brain regions of C57BL/6 mice. The K_d and B_{max} values for each region were calculated from saturation binding experiments, as described under *Experimental Procedures*. Inhibition of [^{3}H]epibatidine (500 pM) binding by cytisine and α-CtxMII was determined as illustrated in Figure 4. Cytisine inhibition was fitted to a two-site model, with IC_{50} and B_{max} values for the less-sensitive binding site being used to calculate the inhibition binding constant (K_i) and size of the cytisine-resistant [^{3}H]epibatidine binding site population in each region. A one-site model was used to determine the K_i values and numbers of α-CtxMII sensitive binding sites in each region. The K_i value of α-CtxMII inhibition of [^{3}H]epibatidine binding did not vary significantly between regions (one-way ANOVA; $F(6,13) = 2.64$, $P > .05$). All values are the mean ± S.E. of values derived from three to four independent experiments.

Region	Total [^{3}H]Epibatidine Binding Population	α-CtxMII-Sensitive Population	K_i (α-CtxMII)	% α-CtxMII-Sensitive	Cytisine-Resistant Population	% Cytisine-Resistant
	fmol/mg of protein		*nM*		*fmol/mg of protein*	
Superior colliculus	259 ± 5	67 ± 6	0.96 ± 0.3	25.9	84 ± 14	32.1
Thalamus	226 ± 5	26 ± 4	5.3 ± 2.8	11.5	39.5 ± 2.6	17.5
Striatum	118 ± 4	16 ± 1	0.83 ± 0.01	13.6	16 ± 2	13.6
Inferior colliculus	123 ± 5	15 ± 1	7.0 ± 1.3	12.2	39 ± 1	31.7
Olfactory tubercles	64 ± 5	14 ± 4	1.1 ± 0.1	21.9	11 ± 1	17.2
Midbrain	159 ± 8	13 ± 1	2.4 ± 1.0	8.2	14 ± 1	8.8
Cortex	62 ± 5	5 ± 2	1.3 ± 0.4	8.1	8 ± 1	12.8
Hippocampus	68 ± 4	N.D.	N/A	None	4 ± 1	5.9
Cerebellum	20 ± 2	N.D.	N/A	None	7 ± 3	35.0
Olfactory bulbs	26 ± 8	N.D.	N/A	None	13 ± 4	50.0
Hindbrain	91 ± 4	N.D.	N/A	None	18 ± 9	19.8
Interpeduncular nucleus	973 ± 154	N.D.	N/A	None	607 ± 34	62.4

N.D., not detectable; N/A, not applicable.

dine binding was found in nuclei innervated by regions where α3 hybridization can be detected (nAChRs are known to be transported from the ventral tegmental area and substantia nigra to the striatum, frontal cortex, olfactory tubercles, and nucleus accumbens (Schwartz et al., 1984), from the retina to the superior colliculus and the geniculate nuclei (Swanson et al., 1987), and from the medial habenula to the interpeduncular nucleus (Clarke et al., 1986). In addition, cytisine-resistant [^{3}H]epibatidine binding was detectable on fiber tracts in the fasciculus retroflexus, oculomotor nerve, optic tract, brachium of the superior colliculus, and supraoptic decussation. Small amounts of α3 hybridization were also found in a number of regions that have no apparent cytisine-resistant [^{3}H]epibatidine binding, most notably the motor trigeminal nucleus and somatosensory cortex.

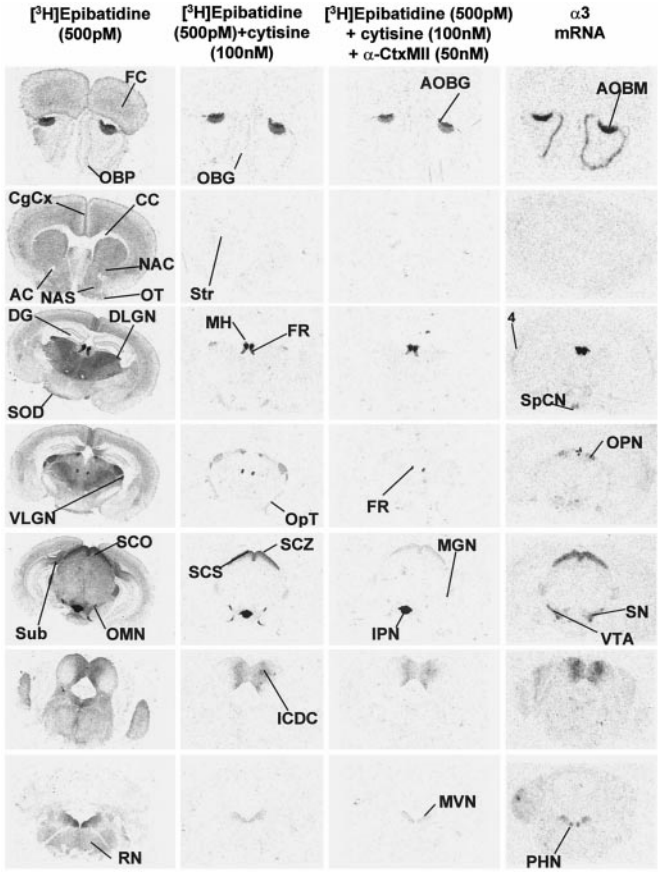

Fig. 5. Autoradiographic comparison of total [^{3}H]epibatidine (500 pM) binding with that in the presence of cytisine (100 nM) or cytisine (100 nM) + α-CtxMII (50 nM) and α3 mRNA expression in mouse brain. Sections (14 μm) were incubated in the presence of 500 pM [^{3}H]epibatidine (left column), 500 pM [^{3}H]epibatidine + 100 nM cytisine (center-left column), 500 pM [^{3}H]epibatidine + 100 nM cytisine + 50 nM α-CtxMII (center-right column), or were subjected to α3 mRNA in situ hybridization (α3 mRNA; right column) as described under *Experimental Procedures*. Nonspecific labeling was indistinguishable from film background. Panels are digital images of autoradiograms. The sections in each row are adjacent. Abbreviations for the indicated brain regions are: 4, somatosensory cortex layer four; AC, anterior commissure; AOBG, accessory olfactory bulb glomerular layer AOBM, accessory olfactory bulb mitral layer; CC, corpus callosum; CgCx, cingulate cortex; DG, dentate gyrus; DLGN, dorsolateral geniculate nucleus; FR, fasciculus retroflexus; FC, frontal cortex; ICDC, inferior colliculus, dorsal cortex; IPN, interpeduncular nucleus; LH, lateral habenula; MGN, medial geniculate nucleus; MH, medial habenula; MVN, medial vestibular nucleus; NAC, nucleus accumbens core; NAS, nucleus accumbens shell; OBG, olfactory bulb glomerular layer; OBP, olfactory bulb internal plexiform layer; OMN, oculomotor nerve (or root); OPN, olivary pretectal nucleus; Opt, optic tract; OT, olfactory tubercle; PHN, prepositus hypoglossal nucleus; RN, reticular nuclei; SCO, superior colliculus, optic nerve layer; SCS, superior colliculus, superficial gray; SCZ, superior colliculus, zonal layer; SN, substantia nigra; SOD, supraoptic decussation; SpCN suprachiasmatic nucleus; Str, striatum; Sub, subiculum; VLGN, ventrolateral geniculate nucleus; VTA, ventral tegmental area.

Discussion

α-CtxMII, originally isolated from the venom of the predatory cone snail, *C. magus* (Cartier et al., 1996), has been used to investigate the diversity of nicotinic receptor binding sites in mouse brain. The data presented here demonstrate that mouse brain high-affinity epibatidine binding has three components: 1) a component that corresponds to the (−)-[^{3}H]nicotine- and [^{3}H]cytisine-binding sites ["cytisine-sensitive" sites, probably the α4β2 subtype (Whiting and Lindstrom, 1987; Flores et al., 1992)] and two sites with lower cytisine affinity ("cytisine-resistant" sites); 2) a cytisine-resistant component that displays high affinity for α-CtxMII and that has been visualized here using ^{125}I-α-CtxMII; 3) a cytisine-resistant component that displays lower affinity for α-CtxMII. This subdivision of mouse brain [^{3}H]epibatidine-binding nAChRs is illustrated in Fig. 7.

^{125}I-α-CtxMII Binds to a Novel nAChR Population. Competition binding experiments demonstrated that α-CtxMII has a low affinity (K_i >10 μM) at mouse brain (−)-[^{3}H]nicotine and ^{125}I-α-Bgt binding sites (Fig. 4). This shows that it binds to a novel neuronal nAChR population, distinct from the well- characterized (−)-[^{3}H]nicotine- and ^{125}I-α-Bgt-binding sites (corresponding to α4β2 and α7-containing subtypes in mammalian neurons; Whiting and Lindstrom, 1987; Schoepfer et al., 1990; Flores et al., 1992; Seguela et al., 1992).

Competition binding experiments using ^{125}I-α-CtxMII in tissue slices yielded K_i values versus ^{125}I-α-CtxMII for unlabeled epibatidine and cytisine of 80 to 90 pM and 14 to 18 nM, respectively. These values are similar to those reported by Marks et al. (1998) for cytisine-resistant [^{3}H]epibatidine-binding sites. As shown in Fig. 3, the cytisine sensitivity of ^{125}I-α-CtxMII-binding sites was constant across brain regions, suggesting that they represent a single population (an alternate but less likely explanation is that multiple sites with a mean cytisine K_i of 20 nM exist in all ^{125}I-α-CtxMII-binding regions). Additionally, ^{125}I-α-CtxMII binding sites have no appreciable affinity for α-Bgt (no displacement by 1 μM α-Bgt) and have a relatively low affinity for (−)-nicotine [K_i = 280–380 nM, compared with 8.9 nM at the mouse brain α4β2 high affinity [^{3}H]nicotine binding subtype (Marks et al., 1998)].

Quantitative autoradiographic analysis showed that specific ^{125}I-α-CtxMII binding occurs in discrete nuclei distributed throughout the mouse brain. The sites' regional distribution is unlike previously reported nicotinic binding patterns and seemed to represent a subset of the cytisine-resistant [^{3}H]epibatidine binding sites reported by Marks et al. (1998). The unusual distribution and nicotinic pharmacology of ^{125}I-α-CtxMII-binding sites confirms that they represent a novel native neuronal nAChR subtype.

α-CtxMII-Binding nAChRs are a Subset of Cytisine-Resistant [^{3}H]Epibatidine Binding Sites. Confirming the data provided by the ^{125}I-α-CtxMII autoradiography experiments, α-CtxMII was a potent inhibitor (mean K_i = 2.7 nM)

of a *fraction* of [^{3}H]epibatidine binding sites in mouse brain regional homogenates (Fig. 4; Table 2). Densities of these α-CtxMII-sensitive [^{3}H]epibatidine-binding sites varied among brain regions, in many cases having a lower density than cytisine-resistant [^{3}H]epibatidine binding sites. Indeed, quantitative autoradiography (Fig. 5) showed that α-CtxMII-sensitive sites are a subset of the cytisine-resistant [^{3}H]epibatidine-binding sites described by Marks et al. (1998).

Quantitative autoradiography showed that the majority of [^{3}H]epibatidine binding sites in mouse brain were highly cytisine-sensitive (Fig. 5, column 1 versus column 2). The distribution of the cytisine-sensitive sites mirrored that reported previously (Marks et al., 1998) and corresponded to the distribution of high affinity nicotine or cytisine binding (Perry and Kellar, 1995; Marks et al., 1998). The autoradiograms demonstrated that these sites were confined to a lim-

TABLE 3

Regional distribution of specific [^{3}H]epibatidine binding [total, + cytisine (100 nM), and + cytisine (100 nM) + α-CtxMII (50 nM)]

Sections (14 μm) were incubated in the presence of 500 pM [^{3}H]epibatidine (total [^{3}H]epibatidine), 500 pM [^{3}H]epibatidine + 100 nM cytisine or 500 pM [^{3}H]epibatidine + 100 nM cytisine + 50 nM α-CtxMII. Binding of [^{3}H]epibatidine was detected by exposing βmax ^{3}H-sensitive film to the sections, followed by digital densitometry of the resultant autoradiograms. Specific binding was calculated by reference to ^{3}H-containing tissue paste standards, and is presented in terms of femtomoles of [^{3}H]epibatidine bound per milligram of tissue weight. The amount of α-CtxMII-sensitive [^{3}H]epibatidine binding in each region was calculated as the difference between the [^{3}H]epibatidine binding in the presence of cytisine (100 nM) alone and that with both cytisine (100 nM) and α-CtxMII (50 nM) present. Six individual measurements were made from each region, under each condition in each mouse where possible. Each value represents the mean ± S.E. of binding measured in three different mice.

	Total [^{3}H]Epibatidine Binding	[^{3}H]Epibatidine Binding with Cytisine (100 nM)	% Total Binding in Presence of Cytisine	[^{3}H]Epibatidine Binding with Cytisine (100 nM) + α-CtxMII-(50 nM)	% Total Binding in Presence of Cytisine + α-CtxMII	α-CtxMII (50 nM) Sensitive [^{3}H]Epibatidine Binding	% α-CtxMII-Resistant (of Cytisine-Resistant)
	fmol/mg protein wet wt.			*fmol/mg protein wet wt.*		*fmol/mg protein wet wt.*	
Telencephalon							
Neocortex							
Cingulate cortex	18.4 ± 1.8	N.D.	None	N.D.	N/A	None	N/A
Frontal cortex	16.0 ± 1.6	0.2 ± 0.1	1.0	N.D.	0None	0.2 ± 0.1	100
Olfactory tubercles	13.7 ± 0.8	2.7 ± 0.3	19.7	0.5 ± 0.3	18.5	2.2 ± 0.01	81.5
Olfactory bulbs							
Accessory olfactory bulbs, glomerular layer	82.2 ± 8.7	66.7 ± 2.7	81.1	48.6 ± 1.7	72.8	18.1 ± 2.5	27.2
Accessory olfactory bulbs, mitral cell layer	37.6 ± 2.7	30.1 ± 0.9	80.0	21.5 ± 1.8	71.6	8.5 ± 1.3	28.4
Olfactory bulbs, glomerular layer	5.7 ± 0.5	2.2 ± 0.4	38.8	2.0 ± 0.3	88.9	0.2 ± 0.1	11.1
Olfactory bulbs, internal plexiform layer	6.6 ± 0.5	2.1 ± 0.3	31.3	1.8 ± 0.3	85.1	0.3 ± 0.1	14.9
Basal ganglia							
Nucleus accumbens, core	15.7 ± 0.8	2.3 ± 0.3	14.4	0.6 ± 0.3	25.9	1.7 ± 0.1	74.1
Nucleus accumbens, shell	13.4 ± 0.5	1.4 ± 0.4	10.7	0.4 ± 0.2	26.8	1.0 ± 0.2	73.2
Striatum	17.2 ± 0.7	1.4 ± 0.3	8.0	0.4 ± 0.2	30.0	1.0 ± 0.1	70.0
Substantia nigra	29.8 ± 1.7	3.3 ± 0.1	10.9	1.8 ± 0.9	56.3	1.4 ± 0.9	43.8
Ventral tegmental area	32.3 ± 2.3	3.5 ± 0.4	10.9	1.1 ± 0.5	33.1	2.3 ± 0.9	66.9
Septum							
Lambdoid septal zone	12.7 ± 0.3	1.2 ± 0.2	9.1	0.2 ± 0.1	18.7	0.8 ± 0.2	81.3
Hippocampus							
Dentate gyrus	14.1 ± 0.8	N.D.	None	N.D.	N/A	None	N/A
Subiculum	43.5 ± 1.3	0.7 ± 0.3	1.6	N.D.	None	0.7 ± 0.3	100
Diencephalon							
Thalamus							
Anteroventral thalamic nucleus	71.7 ± 4.0	4.5 ± 0.4	6.3	3.7 ± 0.1	82.5	0.8 ± 0.5	17.5
Metathalamus							
Dorsolateral geniculate nucleus	69.4 ± 6.1	13.3 ± 0.6	19.3	3.1 ± 0.3	23.6	10.2 ± 0.6	76.4
Medial geniculate nucleus	39.3 ± 2.2	6.6 ± 0.8	16.7	3.5 ± 0.7	53.9	3.1 ± 0.5	46.1
Olivary pretectal nucleus	79.0 ± 6.1	21.0 ± 1.1	26.6	3.4 ± 0.2	16.2	17.6 ± 0.9	83.8
Ventrolateral geniculate nucleus	59.4 ± 5.1	15.5 ± 0.3	26.0	3.1 ± 0.2	20.2	12.3 ± 0.5	79.8
Epi- and subthalamus							
Lateral habenula	69.6 ± 7.0	41.8 ± 5.4	60.0	31.9 ± 1.7	76.4	9.9 ± 3.8	23.6
Medial habenula	380.2 ± 14.5	251.5 ± 20.7	66.1	214.3 ± 4.0	85.2	37.2 ± 16.9	14.8
Mesencephalon							
Inferior colliculus, dorsal cortex	28.3 ± 0.1	10.8 ± 1.0	38.3	7.6 ± 0.6	70.5	3.2 ± 0.6	29.5
Interpeduncular nucleus	308.1 ± 8.9	185.1 ± 15.2	60.1	139.9 ± 4.9	75.6	45.2 ± 10.3	24.4
Superior colliculus, optic nerve layer	28.4 ± 1.0	3.1 ± 0.42	10.9	1.4 ± 0.3	44.6	1.7 ± 0.4	55.4
Superior colliculus, superficial grey	49.1 ± 1.9	16.3 ± 2.0	33.2	3.9 ± 0.5	24.2	12.3 ± 2.2	75.8
Superior colliculus, zonal layer	70.9 ± 2.6	33.8 ± 1.9	47.7	7.4 ± 0.3	22.0	26.4 ± 2.0	78.0
Pons							
Medial vestibular nucleus	23.1 ± 1.3	7.4 ± 0.6	31.9	5.1 ± 0.8	68.8	2.3 ± 0.2	31.2
Prepositus hypoglossal nucleus	25.2 ± 1.7	8.2 ± 1.0	32.5	6.3 ± 0.8	76.8	1.9 ± 0.4	23.2
Pontine nuclei	22.3 ± 2.1	N.D.	None	N.D.	N/A	None	N/A
Reticular nuclei	8.1 ± 0.3	0.3 ± 0.2	3.7	N.D.	None	0.3 ± 0.2	100
Fiber tracts							
Anterior commissure, anterior	2.7 ± 0.6	N.D.	None	N.D.	N/A	None	N/A
Corpus callosum	2.4 ± 0.2	N.D.	None	N.D.	N/A	None	N/A
Fasciculus retroflexus	98.6 ± 7.7	64.8 ± 4.3	65.7	48.4 ± 7.0	74.7	16.4 ± 10.2	25.3
Oculomotor nerve (or root)	74.6 ± 6.4	43.4 ± 4.4	58.2	6.6 ± 0.5	15.2	36.8 ± 4.0	84.8
Optic tract/brachium superior colliculus	15.7 ± 1.2	4.8 ± 0.5	30.6	1.0 ± 0.4	21.8	3.7 ± 0.4	78.2
Supraoptic decussation	17.5 ± 1.9	5.5 ± 0.5	31.3	0.8 ± 0.2	14.7	4.7 ± 0.3	85.3

N.D., not detectable; N/A, not applicable.

ited set of nuclei, scattered throughout the brain. Some (but not all) cytisine-resistant [^{3}H]epibatidine binding was highly α-CtxMII-sensitive (Fig. 5, column 3 versus column 2). The ability of unlabeled α-CtxMII (50 nM) to selectively displace [^{3}H]epibatidine from some cytisine-resistant populations, but not others, further confirms that α-CtxMII interacts only with a subset of cytisine-resistant [^{3}H]epibatidine-binding sites.

The regional densities of ^{125}I-α-CtxMII-binding sites and α-CtxMII-sensitive [^{3}H]epibatidine-binding sites were compared directly (Fig. 6). The distributions of specific ^{125}I-α-CtxMII and α-CtxMII-sensitive [^{3}H]epibatidine-binding sites largely coincided, but numbers of ^{125}I-α-CtxMII-binding sites were consistently lower that those α-CtxMII-sensitive [^{3}H]epibatidine-binding sites. This occurred because a saturating [^{3}H]epibatidine concentration was used, whereas [^{125}I]αCtxMII was used at a concentration below its K_d value. However, in six regions more α-CtxMII-sensitive [^{3}H]epibatidine binding was found than would be predicted from the density of ^{125}I-α-CtxMII binding sites (Fig. 6). This finding needs to be interpreted with some caution: all of these regions contained high levels of [^{3}H]epibatidine binding, and the additional α-CtxMII-sensitive [^{3}H]epibatidine binding sites represent a small portion of total binding. However, if the discrepancy is real, it may represent evidence for a second α-CtxMII-sensitive [^{3}H]epibatidine-binding nAChR population in a small number of nuclei. A relatively high unlabeled α-CtxMII concentration (50 nM) was used to displace [^{3}H]epibatidine binding, so these putative sites could have a relatively low affinity for α-CtxMII (making it undetectable by direct binding of 0.5 nM ^{125}I-α-CtxMII). Thus, although α-CtxMII displays good selectivity for its primary site of action versus [^{3}H]nicotine and ^{125}I-α-Bgt binding sites, high concentrations may distinguish less well between subtypes of cytisine-resistant [^{3}H]epibatidine binding. As a result, it is uncertain whether ^{125}I-α-CtxMII binding to the medial habenula/interpeduncular nucleus tract reflects faint cross-labeling to the high density of other cytisine-resistant [^{3}H]epibatidine binding sites, or the expression of a minor ^{125}I-α-CtxMII binding population.

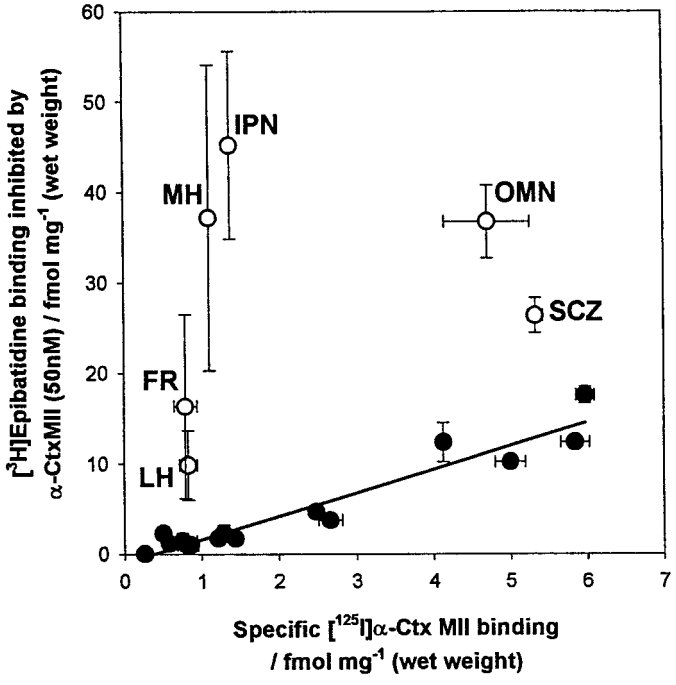

Fig. 6. Comparison of specific ^{125}I-α-CtxMII binding and [^{3}H]epibatidine binding sensitive to α-CtxMII (50 nM) in mouse brain. Amounts of specific ^{125}I-α-CtxMII (0.5 nM) binding were determined in 23 different brain regions by quantitative autoradiography. The amount of α-CtxMII-sensitive [^{3}H]epibatidine binding was quantified in the same regions as the difference between [^{3}H]epibatidine binding in the presence of cytisine (100 nM) and cytisine (100 nM) + α-CtxMII (50 nM). Each point is the mean ± S.E.M. of data gathered from three different animals. In regions with small or zero cytisine- + α-Ctx-MII-resistant [^{3}H]epibatidine binding populations (filled symbols), linear regression showed r = 0.96, slope = 2.6. Those regions containing large amounts of α-CtxMII-resistant [^{3}H]epibatidine binding (open symbols) deviated markedly above the regression line. Abbreviations for the indicated brain regions are: FR, fasciculus retroflexus; IPN, interpeduncular nucleus; LH, lateral habenula; MH, medial habenula; OMN, oculomotor nerve (or root); SCZ, superior colliculus zonal layer.

Physiological Relevance of α-CtxMII-Binding nAChRs. Although α-CtxMII binding nAChRs are relatively rare, they probably exert important physiological effects. α-CtxMII inhibits a component of nicotine-evoked mouse striatal synaptosomal [^{3}H]dopamine release with an IC_{50} value of 2 nM (Grady et al., 1997), similar to the binding affinity reported here (K_i versus [^{3}H]epibatidine = 2.7 nM). Similar IC_{50} values have also been reported for α-CtxMII inhibition

TABLE 4

Regional quantification of α3 mRNA

Data show in situ hybridization of ^{35}S-cRNA for α3 in mouse brain regions. Hybridization was performed as described under *Experimental Procedures*. Hybridized probe was detected by exposing βmax film to the sections, followed by digital densitometry of the autoradiographic images. Specific hybridization was quantified by reference to dot-blotted samples of ^{35}S-cRNA probe of known activity and is presented in terms of pCi/mm^2. Where possible, measurements were made six times in each region, in each mouse. Values are the mean ± S.E. of binding measured in three different mice.

	α3 Hybridization Signal/ pCi/mm^2
Telencephalon	
Neocortex	
Somatosensory cortex, layer IV	2.6 ± 0.4
Olfactory bulbs	
Accessory olfactory bulbs, mitral cell layer	10.0 ± 0.3
Olfactory bulbs, internal plexiform layer	2.4 ± 0.2
Basal ganglia	
Substantia nigra	3.2 ± 0.2
Ventral tegmental area	1.4 ± 0.1
Diencephalon	
Thalamus	
Anteroventral thalamic nucleus	1.5 ± 0.2
Mediodorsal thalamic nucleus	2.0 ± 0.6
Parataenial thalamic nucleus	1.8 ± 0.4
Rostral interstitial nucleus	0.7 ± 0.2
Metathalamus	
Medial geniculate nucleus	2.2 ± 0.3
Olivary pretectal nucleus	1.4 ± 0.1
Epi- and subthalamus	
Medial habenula	47.8 ± 7.7
Parasubthalamic nucleus	0.6 ± 0.2
Hypothalamus	
Arcuate hypothalamic nucleus	1.9 ± 0.4
Medial mamillary nucleus	0.8 ± 0.1
Suprachiasmatic nucleus	1.7 ± 0.3
Mesencephalon	
Central grey, α	0.8 ± 0.2
Central grey, β	2.4 ± 0.3
Inferior colliculus, dorsal cortex	1.8 ± 0.1
Interpeduncular nucleus	1.6 ± 0.3
Superior colliculus, superficial layers	2.8 ± 0.1
Pons	
Locus ceruleus	0.7 ± 0.1
Medial vestibular nucleus	1.2 ± 0.2
Motor trigeminal nucleus	2.9 ± 0.2
Prepositus hypoglossal nucleus	1.4 ± 0.4

of functional responses in rat and avian preparations (Kulak et al., 1997; Ullian et al., 1997; Kaiser et al., 1998). The similar affinities for binding and functional measures strongly imply a competitive mode of antagonism for α-CtxMII in these preparations. Although less than 15% of [^{3}H]epibatidine binding in mouse striatum is α-CtxMII-sensitive, about 50% of nicotine-evoked [^{3}H]dopamine release is inhibited by α-CtxMII (Grady et al., 1997). This disproportionate α-CtxMII sensitivity may arise because of preferential α-CtxMII-sensitive nAChR location on dopaminergic termini.

Identity of α-CtxMII-Binding nAChRs. Marks et al. (1998) noted a resemblance between the patterns of α3 nAChR subunit mRNA expression and cytisine-resistant [^{3}H]epibatidine binding in mouse brain. Direct comparison of the two measures in brain slices prepared from the same animals reinforced this initial impression (Fig. 5). The highest densities of both α3 hybridization and cytisine-resistant [^{3}H]epibatidine binding are found in the medial habenula and accessory olfactory bulbs, and in many nuclei α3 hybridization and cytisine-resistant binding are completely superimposed. The majority of the remaining cytisine-resistant binding sites are found in regions known to be innervated by α3 mRNA expressing regions. Cytisine-resistant nAChRs may also contain other subunits: for instance, the α6 subunit is extensively coexpressed with α3 in rat brain (LeNovere et al., 1996), and Vailati et al. (1999) have shown that α6-containing nAChRs also represent a class of cytisine-resistant nAChRs (K_i values versus [^{3}H]epibatidine binding for cytisine and epibatidine = 11 nM and 20 pM, respectively). nAChRs containing α6 also bind α-CtxMII with moderate affinity (K_i versus [^{3}H]epibatidine = 66 nM), making them possible candidates for the putative second, lower affinity α-CtxMII-binding site discussed previously.

Further evidence supports the involvement of α3 subunits in α-CtxMII-binding sites. α-CtxMII is a selective antagonist of heterologously expressed rat α3β2 nAChRs in *X. laevis* oocytes (Cartier et al., 1996) and human α3β2 in human embryonic kidney 293 cells (Crona et al., 1997). Parker et al. (1998) showed that *X. laevis* oocyte-expressed rat α3β2 nAChRs bind [^{3}H]epibatidine with high affinity and have a low cytisine affinity. Furthermore, the pattern of α-CtxMII-sensitive [^{3}H]epibatidine binding was similar to that described by Schultz et al. (1991) for α-Bgt-insensitive [^{125}I]neuronal Bgt binding. Although neuronal Bgt exhibits complex kinetics of interaction at a variety of nAChR subtypes (Papke et al., 1993), it is a comparatively selective antagonist of heterologously expressed α3β2 nAChRs (Luetje et al., 1990). Together, these data suggest that mouse brain α-CtxMII-sensitive [^{3}H]epibatidine binding occurs at receptors containing α3 and β2 subunits.

The remaining cytisine-resistant [^{3}H]epibatidine binding was found in regions expressing high levels of both the α3 and β4 nAChR subunits (Dinelly-Miller and Patrick, 1992). Again, Parker et al. (1998) report that α3β4-subtype nAChRs bind [^{3}H]epibatidine with detectable affinity and exhibit low cytisine affinity. Thus, it is possible that in mouse brain, the sites less sensitive to α-CtxMII cytisine-resistant binding are a combination of (minimally) α3 and β4 subunits.

In conclusion, this study shows that α-CtxMII is a potent, selective, competitive antagonist at a novel population of mouse brain nAChRs. ^{125}I-α-CtxMII was used in this study to quantify the high α-CtxMII affinity population and map its distribution. Selective inhibition with cytisine and α-CtxMII revealed high affinity [^{3}H]epibatidine binding at three nAChR pharmacological subtypes. The largest [^{3}H]epibatidine binding population was highly cytisine-sensitive and corresponds to the high affinity (−)-[^{3}H]nicotine binding, α4β2 nAChR subtype. Cytisine-resistant sites are likely to be α3 subunit-containing and exhibited differential α-CtxMII sensitivity that may be caused by differing β subunit composition.

Mouse CNS subunits: α2-α7, β2-β4.

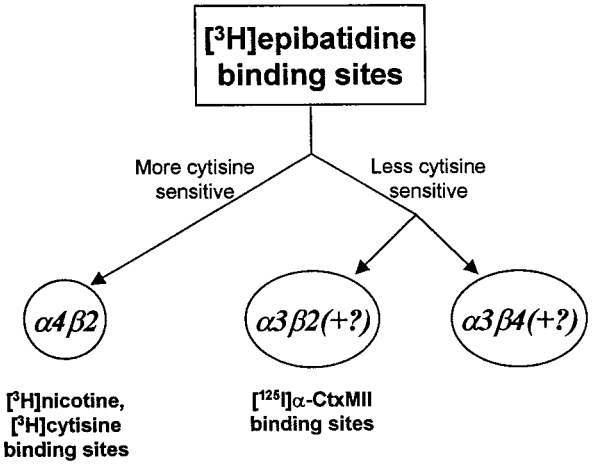

Fig. 7. Summary of [^{3}H]epibatidine binding sites in mouse brain. Using [^{3}H]epibatidine in combination with cytisine reveals that [^{3}H]epibatidine binds specifically and with high affinity in mouse brain to both the well-established (−)-[^{3}H]nicotine and [^{3}H]cytisine binding site of α4β2 composition (Whiting and Lindstrom, 1987; Flores et al., 1992), and a smaller population of nAChRs that are less cytisine sensitive (Marks et al., 1998). This allows the use of cytisine to selectively remove [^{3}H]epibatidine binding at the (−)-[^{3}H]nicotine binding site, revealing sites less sensitive to cytisine binding. The [^{3}H]epibatidine sites that are less cytisine-sensitive are likely to contain the α3 nAChR subunit, and may be divided into two groups according to their α-CtxMII sensitivity. ^{125}I-α-CtxMII may be used to identify and quantify the population that is more α-CtxMII-sensitive and was used in this study to map the distribution of mouse brain high-affinity α-CtxMII binding nAChRs. The population that is more α-CtxMII-sensitive is likely to contain (minimally) α3 and β2 nAChR subunits, whereas the subpopulation that is less α-CtxMII-sensitive can tentatively be assigned a minimal α3 and β4 nAChR subunit composition.

References

Cartier GE, Yoshikami D, Gray WR, Luo S, Olivera BM and McIntosh JM (1996) A new α-conotoxin which targets α3β2 nicotinic acetylcholine receptors. *J Biol Chem* **271:**7522–7528.

Cheng Y-C and Prusoff WH (1973) Relationship between the inhibition constant (K_i) and the concentration of inhibitor which causes 50 per cent inhibition (I_{50}) of an enzymatic reaction. *Biochem Pharmacol* **22:**3099–3108.

Clarke PBS, Hamill GS, Nadi NS, Jacobowitz DM and Pert A (1986) ^{3}H-Nicotine-labeled and ^{125}I-α-Bungarotoxin-labeled nicotinic receptors in the interpeduncular nucleus of rats. 2. Effects of habenular deafferentation. *J Comp Neurol* **251:**407–413.

Cox KH, DeLeon LM, Angerer LM and Angerer RC (1984) Detection of mRNAs in sea urchin embryos by in situ hybridization using asymmetric RNA probes. *Dev Biol* **101:**485–502.

Crona JH, Washburn MS, Stauderman KA, Chavez-Noriega LE, McIntosh JM, Olivera BM, Zhou L-M, McCabe RT, Grant GA, Harpold M and Corey-Naeve J (1997) Characterization of the inhibitory effects of κ-bungarotoxin and α-conotoxin IMI and α-conotoxin MII on human nicotinic receptor-mediated calcium responses and ionic currents. *Soc Neurosci Abstr* **23:**155.6.

Dinelly-Miller K and Patrick J (1992) Gene transcripts for the nicotinic acetylcholine receptor subunit, β4, are distributed in multiple areas of the rat central nervous system. *Mol Brain Res* **16:**339–344.

Flores CM, Rogers SW, Pabreza LA, Wolfe BB and Kellar KJ (1992) A subtype of

nicotinic cholinergic receptor in the brain is composed of α4 and β2 subunits and is upregulated by chronic nicotine treatment. *Mol Pharmacol* **41:**31–37.
Geary WA, Toga AW and Wooten GF (1985) Quantitative film autoradiography for tritium: methodological considerations. *Brain Res* **337:**99–108.
Grady SR, McIntosh JM, Marks MJ and Collins AC (1997) Effects of α-conotoxin MII on nicotine-stimulated dopamine release from mouse striatal synaptosomes. *Soc Neurosci Abstr* **23:**266.20.
Kaiser SA, Soliakov L, Harvey SC, Luetje CW and Wonnacott S (1998) Differential inhibition by α-conotoxin-MII of the nicotinic stimulation of [^{3}H]dopamine release from rat striatal synaptosomes and slices. *J Neurochem* **70:**1069–1076.
Kulak JM, Nguyen TA, Olivera BM and McIntosh JM (1997) α-Conotoxin MII blocks nicotine stimulated dopamine release in rat striatal synaptosomes. *J Neurosci* **17:**5263–5270.
LeNovere N, Zoli M and Changeux J-P (1996) Neuronal nicotinic receptor α6 subunit mRNA is selectively concentrated in catecholaminergic nuclei of the rat brain. *Eur J Neurosci* **8:**2428–2439.
Lindstrom J, Anand R, Gerzanich V, Peng, Wang F and Wells G (1996) Structure and function of neuronal nicotinic acetylcholine receptors. *Prog Brain Res* **109:**125–137.
Lowry A, Rosebrough NJ, Farr AL and Randall RJ (1951) Protein measurement with the Folin phenol reagent. *J Biol Chem* **193:**263–275.
Luetje CW, Wada K, Rogers S, Abramson SN, Tsuji K, Heinemann S and Patrick J (1990) Neurotoxins distinguish between different neuronal nicotinic acetylcholine receptor subunit combinations. *J Neurochem* **55:**632–640.
Marks MJ, Pauly JR, Gross SD, Deneris ES, Hermans-Borgmeyer I, Heinemann SF and Collins AC (1992) Nicotine binding and nicotinic receptor subunit mRNA after chronic nicotine treatment. *J Neurosci* **12:**2765–2784.
Marks MJ, Smith KW and Collins AC (1998) Differential agonist inhibition identifies multiple epibatidine binding sites in mouse brain. *J Pharmocol Exp Ther* **285:**377–386.
Marks MJ, Stitzel JA, Romm E, Wehner JM and Collins AC (1986) Nicotinic binding sites in rat and mouse brain: comparison of acetylcholine, nicotine and α-bungarotoxin. *Mol Pharmacol* **30:**427–436.
Papke RL, Duvoisin RM and Heinemann SF (1993) The amino terminal half of the nicotinic β subunit domain regulates the kinetics of inhibition by neuronal-bungarotoxin. *Proc R Soc Lond B Biol Sci* **252:**141–148.
Parker MJ, Beck A and Luetje CW (1998) Neuronal nicotinic receptor β2 and β4 subunits confer large differences in agonist binding affinity. *Mol Pharmacol* **54:**1132–1139.
Pauly JR, Stitzel JA, Marks MJ and Collins AC (1989) An autoradiographic analysis of cholinergic receptors in mouse brain. *Brain Res Bull* **22:**453–459.
Perry DC and Kellar KJ (1995) [^{3}H]Epibatidine labels nicotinic receptors in rat brain: an autoradiographic study. *J Pharmacol Exp Ther* **275:**1030–1034.
Schoepfer R, Conroy WG, Whiting P, Gore M and Lindstrom J (1990) Brain α-bungarotoxin binding protein cDNAs and mAbs reveal subtypes of this branch of the ligand-gated ion channel gene superfamily. *Neuron* **5:**35–48.
Schulz DW, Loring RH, Aizenman E and Zigmond RG (1991) Autoradiographic localization of putative nicotinic receptors in the rat brain using ^{125}I-neuronal bungarotoxin. *J Neurosci* **11:287–297.**
Schwartz RD, Lehman J and Kellar KJ (1984) Presynaptic nicotinic cholinergic receptors labeled by [^{3}H]acetylcholine on catecholamine and serotonin axons in brain. *J Neurochem* **42:**1495–1498.
Seguela P, Wadiche J, Dineley-Miller K, Dani JA and Patrick JW (1992) Molecular cloning, functional properties and distribution of rat brain α7: a nicotinic cation channel highly permeable to calcium. *J Neurosci* **13:**596–604.
Simmons DM, Arriza JL and Swanson LW (1989) A complete protocol for in situ hybridization of messenger RNAs in brain and other tissues with radiolabeled single-stranded RNA probes. *J Histotechnol* **12:**169–181.
Swanson LW, Simmons DM, Whiting PJ and Lindstrom J (1987) Immunohistochemical localization of neuronal nicotinic receptors in the rodent central nervous system. *J Neurosci* **7:**3334–3342.
Ullian EM, McIntosh JM and Sargent PB (1997) Rapid synaptic transmission in the avian ciliary ganglion is mediated by two distinct classes of nicotinic receptors. *J Neurosci* **17:**7210–7219.
Vailati S, Hanke W, Bejan A, Barabino B, Longhi R, Balestra B, Moretti M, Clementi F and Gotti C (1999) Functional α6-containing nicotinic receptors are present in chick retina. *Mol Pharmacol* **56:**11–19.
Whiting P and Lindstrom J (1987) Purification and characterization of nicotinic acetylcholine receptor from rat brain *Proc Natl Acad Sci USA* **84**:595–599.
Wonnacott S (1997) Presynaptic nicotinic ACh receptors. *Trends Neurosci* **20:**92–98

Send reprint requests to: Dr. A.C. Collins, Institute for Behavioural Genetics, University of Colorado, Campus Box 447, Boulder, CO 80303-0447.